Empirical estimates of the mutation rate for an alphabaculovirus

Dieke Boezen[1a], Ghulam Ali[2a,b], Manli Wang[3], Xi Wang[3], Wopke van der Werf[4], Just M. Vlak[2], Mark P. Zwart[1*]

[1] Department of Microbial Ecology, The Netherlands Institute of Ecology (NIOO-KNAW), Wageningen, The Netherlands

[2] Laboratory of Virology, Wageningen University and Research, Wageningen, The Netherlands

[3] Wuhan Institute of Virology, Chinese Academy of Sciences, Wuhan, PR China

[4] Centre for Crop Systems Analysis, Wageningen University and Research, Wageningen, The Netherlands

[a] Equal contribution

[b] Current affiliation: Air University Multan Campus, Khan Centre, 82-Abdali Road, Islamabad, Pakistan

* Correspondence: M.Zwart@nioo.knaw.nl; Tel.: +31 317 473431

Abstract

Mutation rates are of key importance for understanding evolutionary processes and predicting their outcomes. Empirical estimates of mutation rate are available for a number of RNA viruses, but few are available for DNA viruses, which tend to have larger genomes. Whilst some viruses have very high mutation rates, lower mutation rates are expected for viruses with large genomes to ensure genome integrity. Alphabaculoviruses are insect viruses with large genomes and often have high levels of polymorphism, suggesting high mutation rates despite evidence of proofreading activity by the replication machinery. Here, we report an empirical estimate of the mutation rate per base per strand copying (s/n/r) of Autographa californica multiple nucleopolyhedrovirus (AcMNPV). To avoid biases due to selection, we analyzed mutations that occurred in a stable, non-functional genomic insert after five serial passages in *Spodoptera exigua* larvae. Population bottlenecks, viral mode of replication and thresholds for mutation detection likely affect mutation rate estimates, and we therefore used population genetic models that account for these processes to infer the mutation rate. We estimated a mutation rate of 1×10^{-7} s/n/r. This estimate was not sensitive to different model assumptions or including whole genome data. The rates at which different classes of mutations accumulate provide good evidence for neutrality of mutations occurring within the inserted region. We therefore present a robust approach for mutation rate estimation for viruses with stable genomes, and strong evidence of a much lower alphabaculovirus mutation rate than supposed based on the high levels of polymorphism observed.

Author Summary

Virus populations can evolve rapidly, driven by the large number of mutations that occur during virus replication. It is challenging to measure mutation rates because selection will affect which mutations are observed: beneficial mutations are overrepresented in virus populations, while deleterious mutations are selected against and therefore underrepresented. Few mutation rates have been estimated for viruses with large DNA genomes, and there are no estimates for any insect virus. Here, we estimate the mutation rate for an alphabaculovirus, a virus that infects caterpillars and has a large, 134 kilobase pair DNA genome. To ensure that selection did not bias our estimate of mutation rate, we studied which mutations occurred in a large artificial region inserted into the virus genome, where mutations did not affect viral fitness. We deep sequenced evolved virus populations, and compared the distribution of observed mutants to predictions from a simulation model to estimate mutation rate. We found evidence for a relatively low mutation rate, of one mutation in every 10 million bases replicated. This estimate is in line with expectations for a virus with self-correcting replication machinery and a large genome.

35 # Introduction

36 Mutation rates are of key importance for understanding and predicting evolutionary patterns, as
37 the mutation rate modulates the mutation supply of a population [1]. Large mutation supplies can
38 fuel rapid and repeatable adaptation [2,3], but also increase the mutational load on a population
39 [4]. By contrast, low mutation supplies can limit the rate of adaptation [5], but also result in a lower
40 mutational load [4]. The impact of mutational supply also depends on the topography of the fitness
41 landscape. Small mutational supplies can have advantages for evolution on rugged fitness
42 landscapes: although adaptation will be slower and in most cases less fit genotypes will be
43 selected, some populations can avoid becoming trapped on local fitness peaks [6]. Mutation rates
44 are not only relevant to understanding basic evolutionary processes, but they also impinge on
45 real world outcomes, such as the efficacy of prophylactic or therapeutic interventions to infectious
46 diseases [7,8].

47 Viruses have high mutation rates [7,9,10], with estimates of mutations per site per strand
48 copying (s/n/r) ranging from 2×10^{-8} for Enterobacteria phage T2 [11] to 2×10^{-4} for Influenza A virus
49 [12]. Whilst these high mutation rates are thought to contribute to the rapid adaptation of viruses,
50 the majority of mutations are typically deleterious [13,14]. Many viruses with large genomes
51 belong to Group I of the Baltimore classification (dsDNA viruses) [15], and typically have
52 polymerases with proofreading activity, which should enhance the fidelity of replication [16]. A
53 general expectation is therefore that viruses with relatively large genomes have lower mutation
54 rates [9]. An inverse relationship between genome size and mutation rate indeed has been found.
55 Small genomes can tolerate higher mutation rates as a larger proportion of mutation-free
56 genomes are generated in each round of replication, due to their small size [9,17].

57 The alphabaculoviruses are a large group of insect baculoviruses that have been studied
58 because of their biocontrol and biotechnological potential [18,19]. Alphabaculoviruses have

59 relatively large dsDNA genomes compared to other viruses [20], and high levels of within-host
60 genetic diversity have been documented from wild [21–23] and captive [24] insect populations. It
61 has been suggested that baculoviruses might therefore have high mutation rates despite their
62 large genome sizes [24]. To our knowledge, no empirical estimates of the mutation rate have
63 been reported for any baculovirus or insect virus to date, and there are only a few estimates for
64 other large dsDNA viruses [9].

65 A major challenge for making empirical estimates of mutation rates is the need to account
66 for biases due to selection [9]. Studies on the distribution of mutational fitness effects (DMFE)
67 have shown that most mutations in viral genomes are deleterious [13,14], and selection will
68 remove these mutations from populations. By contrast, beneficial mutations will increase in
69 frequency due to selection. These opposing effects of purifying and directional selection make it
70 problematic to derive information on mutation rates directly from mutation accumulation in a viral
71 genome. Many different approaches have been developed to remove the bias introduced by
72 selection [7,9]. For example, some studies considered the frequency of lethal mutations in a
73 population, since these variants cannot replicate autonomously and therefore represent a
74 snapshot of genetic variation [25]. Others have evolved viruses in hosts expressing a viral gene,
75 and then restricting their analysis to the sequence of this redundant viral gene [26]. Another
76 strategy reported recently has been to incorporate fluorescent markers with inactivating mutations
77 into a viral genome, and then performing fluctuation tests based on recovering fluorescence [12].

78 In the current study, we report the first empirical estimate of mutation rate for a large
79 dsDNA virus, the alphabaculovirus Autographa californica multiple nucleopolyhedrovirus
80 (AcMNPV). To ensure selection did not bias our estimates, we analyzed virus populations carrying
81 a large, nonfunctional genomic insert that was stably maintained [27], exploiting the genomic
82 stability of the Group I viruses [28]. For our analysis, we assumed that mutations in this region
83 are neutral due to the absence of known viral genes and regulatory sequences, and verified this

84 assumption. We also developed a population genetics model to estimate mutation rates from
85 empirical data, that incorporates the effects of population bottlenecks and different modes of virus
86 replication on the occurrence and maintenance of mutations. Using this approach, we made
87 robust estimates of the mutation rate for a baculovirus for the first time.

88 # Results and Discussion

89 **Serial passage and detection of mutations**

90 To estimate the mutation rate of a large dsDNA virus, we experimentally evolved a variant of
91 alphabaculovirus AcMNPV containing a stable, non-functional genomic region. The AcMNPV
92 variant used was a so-called bacmid: an infectious clone that also contains the AcMNPV genome
93 (~134 kb). It also contains bacterial sequences that enable propagation as a low copy number
94 plasmid in *Escherichia coli* (~12.5 kb) and the acceptance of expression cassettes by
95 transposition [27]. The specific variant used here contains an expression cassette from the
96 pFastBac-Dual vector to restore expression of complete and functional polyhedrin (Figure 1). We
97 consider the inserted bacterial sequences to be non-functional and therefore neutral in insects,
98 except for the polyhedrin promoter and open reading frame (ORF) sequences derived from the
99 pFastBac Dual vector. This renders an 11,646 bp neutral region for a mutation accumulation
100 experiment (Figure 1). By contrast, the remainder of the AcMNPV genome is intact and unaltered,
101 making this system representative for this virus. We will hereafter refer to this bacmid-derived
102 AcMNPV variant with restored polyhedrin expression as “BAC”. The virus could be reconstituted
103 from the infectious clone by transfection of the BAC genome into fourth instar (L4) *Spodoptera*
104 *exigua* (Hübner) (see Materials and Methods). Mutations were allowed to accumulate across the
105 BAC genome by experimentally evolving five replicate BAC lineages (referred to as lineages A,
106 B, C, D and E) for five passages in *S. exigua* L2. For each replicate lineage, passaging was
107 performed in five larvae exposed to a high viral dose of occlusion bodies (OBs) sufficient to kill all
108 larvae. Upon death larval cadavers were collected and pooled prior to the isolation of OBs, which
109 were used to inoculate larvae orally for the next passage. Further details on the experimental
110 evolution experimental setup can be found in the Materials and Methods.

111 Evolved lineages A - E, as well as the ancestral BAC were sequenced using Illumina

112 HiSeq to detect mutations in both the non-functional genomic insert, as well as across the whole
113 baculovirus genome. When mapping reads to the BAC reference genome we noticed a correlation
114 between low sequencing coverage and the calling of mutations, and we therefore removed
115 regions with relatively low coverage (Figures S1-S4, see Materials and Methods). We show that
116 mutations indeed accumulated across lineages and passages (Table 1). When analyzing the
117 sequence data, the number of mutations detected is dependent on the minimum threshold value
118 (τ) for mutation frequency (e.g. τ values of 0.5, 1, 2% were used). Regardless of the chosen
119 mutation frequency threshold, the number of mutations detected is low for both the bacmid insert
120 and genome after five passages in *S. exigua* L2.

121

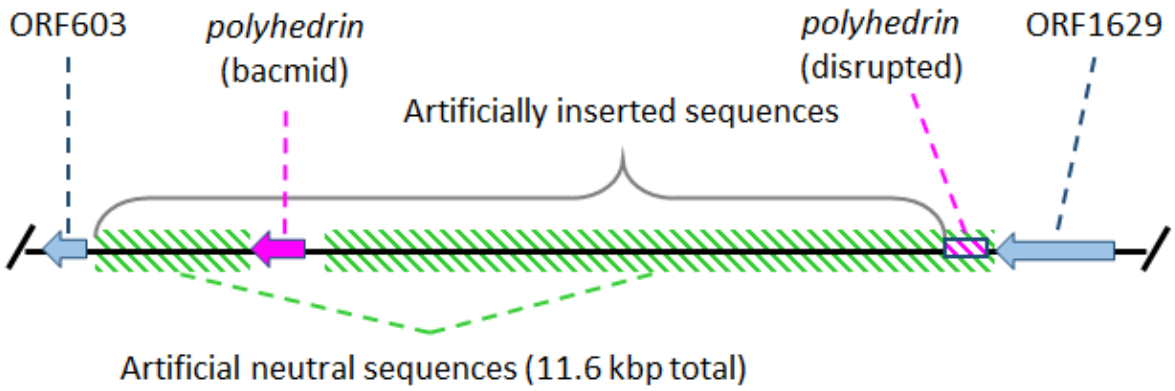

122

123 **Figure 1:** Illustration of the neutral region (green diagonal bars) used for estinating mutation rate
124 . ORF603 and ORF1629 (light blue) are native AcMNPV genes, between which lies the *polyhedrin*
125 gene which was disrupted (box with magenta bars) by the insertion of the bacmid sequences in
126 its 5' end. To restore *polyhedrin* expression the gene has been reinserted under control of its
127 native promotor within the bacmid insert. We consider the sequences of bacterial origin in the
128 insert and the remnants of the pseudogenized *polyhedrin* gene copy as neutral sequences.

129 **Table 1:** Mutations called per lineage, where τ is the threshold frequency for detecting mutations.

	Neutral region only			Whole genome		
Lineage	τ = 0.5%	τ = 1.0%	τ = 2.0%	τ = 0.5%	τ = 1.0%	τ = 2.0%
BAC	1	-	-	1	-	-
A	2	-	-	20	7	1
B	2	-	-	14	3	2
C	1	1	-	9	2	1
D	1	1	-	7	6	2
E	2	1	1	18	2	2

130

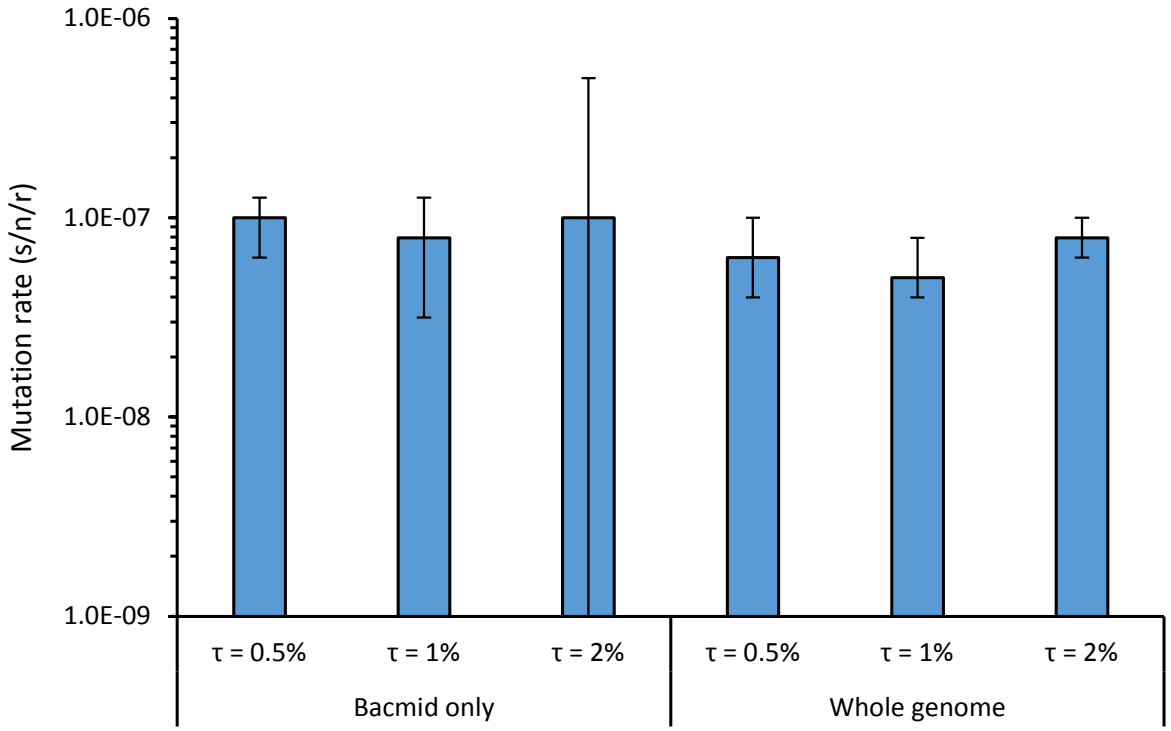

131

132 **Figure 2:** Mutation rate estimates (s/n/r, mutations per site per strand copying) derived with the
133 model are given based on the neutral bacmid region or the whole genome. Different values for
134 the threshold frequency for detecting mutations (τ) were used, noted as percentages here. Error
135 bars represent the 95% fiducial limits, as determined by bootstrapping. Note that for the neutral
136 region and τ = 2.0%, the lower fiducial limit extends to zero due to the low number of mutations
137 detected.

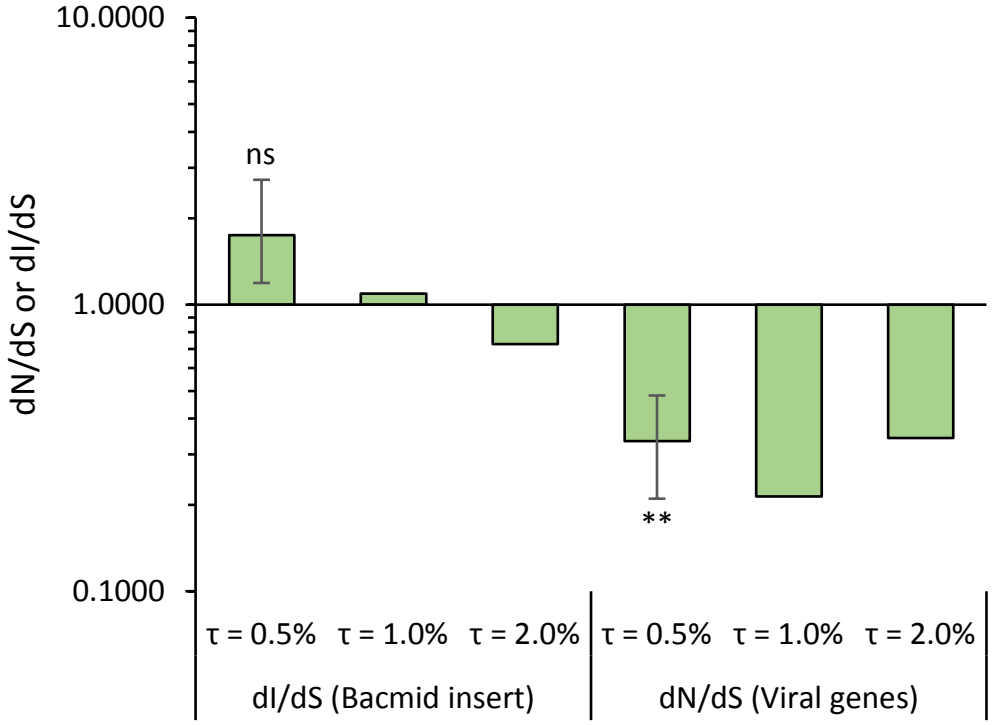

Figure 3: The rate of mutations in the artificial neutral regions (dI), normalized by the rate of synonymous mutations in native viral genes (dS), is shown by the three bars on the left. The values are close to 1, indicating neutral evolution. The three bars on the right show the rate of non-synonymous mutations in viral genes (dN), normalized by dS. These values are less than 1, indicating purifying selection. dI/dS and dN/dS values were determined for different values for the threshold frequency for detecting mutations (τ), noted as a percentage in the figure. Only for the lowest threshold value for mutation detection (τ = 0.5%) were there synonymous mutations detected in each sample, and therefore we could perform statistical analysis only for this condition. Error bars indicate the 95% confidence interval of the estimate as determined by bootstrapping, and results of a one-sample *t*-test are indicated by ns (non-significant, $p > 0.05$) and ** ($P < 0.01$).

151 **Low mutation rate for AcMNPV with bacmid and whole-genome mutation data**

152 To make robust inferences on the mutation rate (μ) from these experimental data, we developed
153 a population genetic model. Briefly, we generated a stochastic model simulating neutral evolution
154 in a virus genome, modelled as mutation frequencies per base per viral generation. We fitted this
155 model to the experimental data by considering the number of bases with a frequency of mutations
156 above the threshold τ, using a maximum likelihood approach. We estimated the viral mutation
157 rate to be ~1×10^{-7} s/n/r, with all estimates for the neutral bacmid region and the whole genome
158 data being similar (Figure 2). Below we describe these results in more detail.

159 The simulation model was run for a range of model parameter values for mutation rate,
160 viral replication modes (ρ values of 1, 3 and 10; see also Materials and Methods section),
161 threshold values for mutation detection (τ values of 0.5%, 1% and 2%), and lengths corresponding
162 to the neutral bacmid region only and the whole virus genome (see Materials and Methods section
163 for details). Strikingly, our mutation rate estimates were robust relative to the replication mode ρ
164 value and to the choice of experimental data used (neutral region or whole genome), with
165 estimates of approximately 1×10^{-7} s/n/r in all scenarios (Figure 2, Figure S5-S6). We also
166 estimated the mutation rate with established models for sequencing data from clones [9], adapting
167 these methods to use the frequency of mutations determined by high-throughput sequencing data
168 instead of Sanger sequences from clones (see Materials and Methods). These estimates were
169 similar to those obtained with the first approach, although they tended to be about a factor 2.5
170 smaller ($\mu \leq 4 \times10^{-8}$ s/n/r, Figure S7). This difference was expected, as this alternative approach
171 does not take into consideration the effects of the mutation detection threshold τ, but rather
172 assumes all mutations will be detected irrespective of their frequency. As the sensitivity limits of
173 the deep-sequencing data is not taken into account, this approach will underestimate the mutation
174 rate.

175 One of the purported strengths of the first approach is that we have a large region (11.6
176 kb) in which point mutations will not affect fitness, given there are no known viral genes or
177 regulatory sequences (Figure 1). Although large genomic deletions in this region would
178 presumably be beneficial as they could speed up viral replication [28], none were detected:
179 Sequence coverage was similar to the rest of the genome for the evolved populations (Figures
180 S1-S4), ruling out the occurrence of large deletions at high frequencies. To test if point mutations
181 in this region were indeed neutral, we considered the rate at which mutations occurred in the
182 neutral intergenic region (dI) normalized by the rate of synonymous substitutions in viral genes
183 (dS) (see Materials and Methods). If mutations in the inserted region are neutral, we expect dI/dS
184 ~ 1. For the different values of τ used, dI/dS estimates were indeed approximately 1 (Figure 3),
185 ranging from 0.72 to 1.96. For the condition under which we could perform a formal test ($\tau > 0.5\%$),
186 dI/dS was not significantly different from 1 (One-sample *t*-test: $t_4 = 1.685$, $p = 0.167$), providing
187 support to the idea that mutations in the bacmid region are neutral. By contrast, when the same
188 analysis was performed for the rate of nonsynonymous mutations (dN) in viral genes, all dN/dS
189 values were ≤ 0.34 (Figure 3). For the condition under which we could perform a formal test ($\tau >$
190 0.5%), dN/dS was significantly lower than 1 ($t_4 = -5.717$, $p = 0.005$). This underrepresentation of
191 nonsynonymous mutations in the viral genome presumably occurs because most
192 nonsynonymous mutations will be deleterious [13,14], and therefore are removed by purifying
193 selection. Despite evidence for purifying selection acting on viral genes, mutation rate estimates
194 were similar for the neutral region and the whole genome (Figure 2).

195 The accumulation of mutations in a virus population is affected by the viral replication
196 mode (ρ) [9,10,29–31], and the distribution of mutation frequencies is linked to the mode of
197 replication [31]. Here we considered this effect by fitting the genome evolution model with values
198 $\rho = 1$ (the "geometric growth" scenario), $\rho = 3$ (mixed replication scenario) and $\rho = 10$ ("stamping
199 machine" scenario). We found that viral mode of replication had a consistent but small effect on

200 the estimated mutation rate (Figure S6), with higher values of ρ corresponding to higher mutation
201 rate estimates, as expected. The effect on model fit was minimal (Figure S5), and we therefore
202 cannot make inferences on the mode of replication from these data. This result is not surprising,
203 given that the number of mutations we detected was small and that the model fitting only considers
204 the number of sites with a mutation frequency above τ, and not the frequency of individual
205 mutations. For baculoviruses, the mode of replication has not been described formally, to the best
206 of or our knowledge. However, as these viruses probably employ rolling circle amplification [32],
207 replication is likely to follow the "stamping machine" scenario and to be described best by high
208 values of ρ.

209 **AcMNPV mutation rate estimate is congruent with estimates for other viruses**

210 Mutation rates (s/n/r) have been estimated for a number of viruses, allowing for a comparison with
211 our baculovirus estimate. For this comparison, we included a collection of mutation rate data
212 [9,33], with updated mutation rates for the RNA viruses influenza A virus [12] and poliovirus [31]
213 due to the availability of better estimates. When multiple mutation rates were available for one
214 virus, we used only the most recent estimate because methodological advances make estimates
215 that are more recent more reliable. Our estimate clearly is congruent with mutation rate estimates
216 for other dsDNA viruses, as it is close to the predicted relationship between genome size and
217 mutation rate (Figure 4). As AcMNPV has a relatively large genome, it is also one of the lowest
218 estimates of mutation rate in DNA viruses reported in the literature, similar to that of Escherichia
219 virus λ, and with only Enterobacteria phage T2 (170 kbp) being lower.

220 Besides being consistent with trends in other viruses, our estimate of mutation rate for
221 AcMNPV is congruent with what is known about its polymerase. AcMNPV codes for a DNA-
222 dependent DNA polymerase (DNApol) that belongs to the family B DNA polymerases and
223 contains the exonuclease domain, thought to be responsible for proofreading and editing of

224 mismatches [16,34,35]. The 3' to 5' exonuclease activity of this domain - essential for repairing
225 errors - has been confirmed [36], and hence a low mutation rate is expected for AcMNPV. The
226 other viruses with low mutation rates are both dsDNA bacteriophages with relatively large
227 genomes (Figure 4). Proofreading activity also has been demonstrated in the case of T2 [37].

228 **Analysis of the mutational spectrum: a low transition to transversion ratio?**

229 We considered whether our data shed light on AcMNPV's mutation spectrum, the occurrence of
230 the different kinds of single-nucleotide mutations, focusing on the transition to transversion ratio
231 (Table 2; see also Table S1). For the neutral region, the number of observed mutations is too
232 small to be informative, even for the lowest mutation detection threshold of τ = 0.5%. For the
233 whole genome and for the lowest mutation detection threshold, transitions are close to the
234 expected ratio in the absence of mutation bias (0.5), which may indicate a low transition to
235 transversion ratio. However, this trend does not hold for higher values of τ, and selection may
236 bias the mutations detected outside of the neutral region. Due to the small number of mutations
237 detected in the neutral bacmid region and the possible effects of selection on the whole-genome
238 data, we therefore cannot draw any firm conclusions on AcMNPV's mutational spectrum. Analysis
239 of a larger number of neutral mutational events will be necessary to draw conclusions on mutation
240 spectrum. These larger numbers could be achieved by analyzing a larger number of replicate
241 populations or populations evolved over a longer period of time, although improved sequencing
242 methods with much lower error rates [38] would probably suffice to analyze mutation bias for the
243 evolved populations described here.

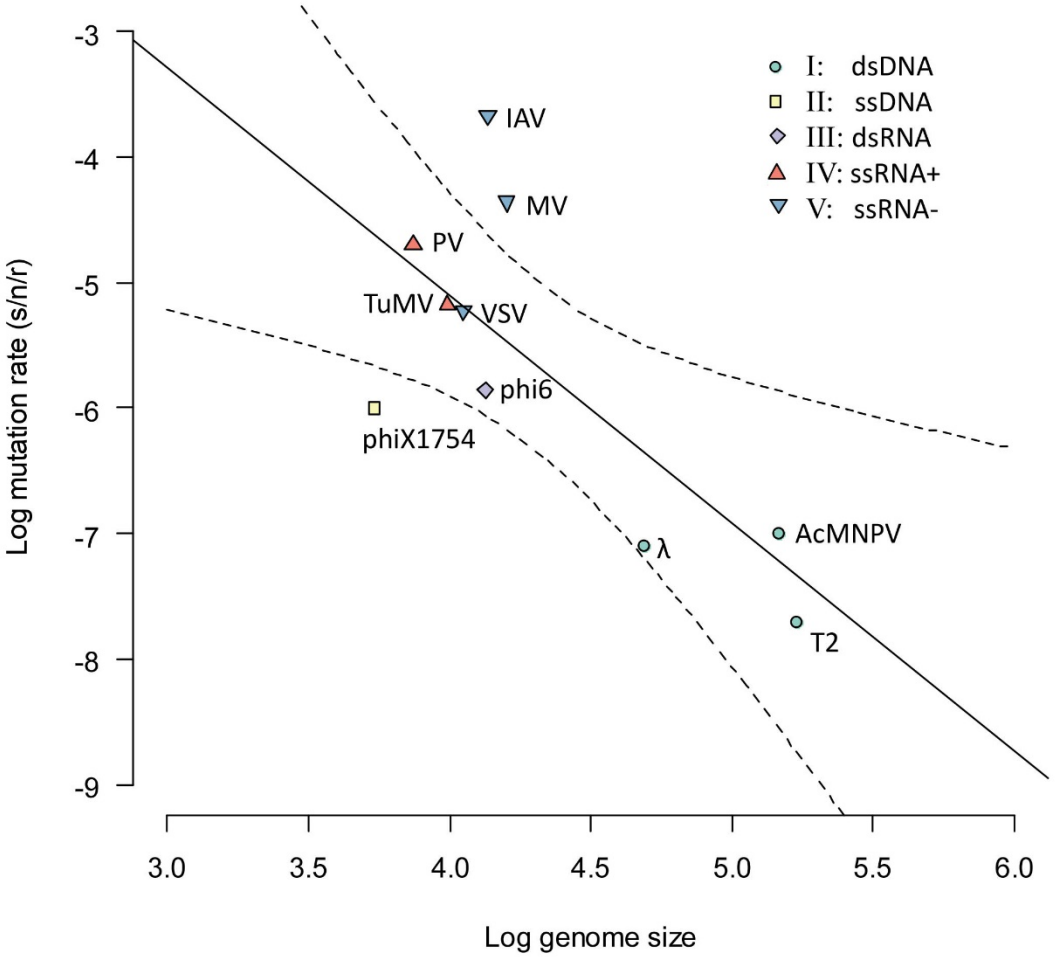

Figure 4: An overview of known mutation rate estimates (s/n/r, ordinate) for viruses with different genome sizes (abscissa) is given. The color and shapes of symbols indicate the Baltimore classification group to which each virus belongs, as indicated by the legend in the top right of the figure. The solid black line marks the regression line, with dotted lines marking the 95% confidence interval. The slope of the fitted relationship is significantly less than zero (t_8 = -3.243, p = 0.012), and the coefficient of determination (r^2) is 0.568. Our mutation rate estimate for AcMNPV is in good agreement with the fitted relationship between genome size and mutation rate. Other virus names in the figure are Enterobacteria phage T2 (T2), Escherichia virus λ (λ), Escherichia virus ΦX174 (phiX174), Influenza A virus (IAH), Measles virus (MV), Poliovirus (PV), Pseudomonas virus Φ6 (Phi6), Turnip mosaic virus (TuMV), and Vesicular stomatitis virus (VSV).

255 **Table 2:** Overview mutation spectrum

	Relative frequency of mutation			
	Whole genome			Bacmid only
Observation or index	$\tau = 0.5$	$\tau = 1.0$	$\tau = 2.0$	$\tau = 0.5$
Transitions / Transversions	28/50	9/11	6/2	4/5
Ratio[a] [95% confidence interval]	0.56 [0.34-0.91]	0.82 [0.30-2.17]	3.00 [0.54-30.3]	0.80 [0.15-3.72]

256 [a] The ratio of transitions to transversions

257 **Concluding remarks**

258 Our low mutation rate estimate is congruent with the large genome size of AcMNPV and its known
259 proofreading activity [36]. By contrast, the high genetic variation often observed within
260 alphabaculovirus populations [21-24] remains a conundrum. In one case frequency-dependent
261 selection has been observed and may account for stable polymorphisms [39,40]. Whether
262 intricate relationships between genetic variants that complement each other are common or
263 evolutionarily stable remains to be seen, but such relationships would help to explain the genetic
264 diversity often seen within alphabaculovirus populations.

265 We estimated the mutation rate for the alphabaculovirus AcMNPV, using a novel approach
266 that depends on the insertion of an artificial neutral region in the viral genome, and which starts
267 with a single genotype and exploits the genome stability of group I dsDNA viruses. Such an
268 approach requires mutations in this 'artificial' region to be neutral, and dI/dS results suggest this
269 assumption is met. Whereas others have employed rolling circle amplification of sequencing
270 templates to reduce sequencing error [38], here we developed an approach to analyzing regular
271 Illumina sequencing data that were not gathered specifically with the intent of determining
272 mutation rates. Our approach relies on a detailed analysis of the sequencing data to eliminate
273 obvious sequencing biases and a comparison of sequencing data to simulation-model predictions.
274 The use of models allows us to take into consideration the effects of viral demography on mutation
275 rate estimates, and also limit the impact of choosing thresholds for mutation detection, as the
276 same threshold is applied in the model.

277 # Materials and Methods

278 *Experimental evolution of AcMNPV*

279 pBac-E2 (BAC) was evolved experimentally in *S. exigua* larvae in five replicate lineages (A, B, C,
280 D and E). To reconstitute the virus from the bacmid, the haemocoel of *S. exigua* L4 was injected
281 with a total volume of 20 µl (i.e., 2 × 10 µl), containing a 4:1:1 mixture of Lipofectin transfection
282 reagent (ThermoFisher Scientific), water and BAC DNA (~ 15 µg DNA per larva). Upon larval
283 death, OBs were harvested from cadavers. From a single infected larva, OBs were isolated and
284 diluted to $2x10^7$ OBs/ml. Serial passage of BAC was performed five times for each replicate
285 lineage, with five larvae used for each replicate lineage. For each passage, newly molted L2 were
286 starved for 12 h and then inoculated by droplet feeding with an OB suspension exceeding 10 x
287 LC_{99} (≥ $2x10^7$ OBs/ml), to avoid narrow transmission bottlenecks. Per replicate lineage, five
288 inoculated larvae were transferred to 6-well tissue culture plates with artificial diet plugs. Larvae
289 were incubated at 26°C and with a 14 h:10 h day-night photoperiod. Upon death, larval cadavers
290 were collected, pooled and used to inoculate the next passage. After five passages, lineages A -
291 E were amplified using 100 *S. exigua* L3, and 1.5×10^9 OBs were used to extract viral genomic
292 DNA. Briefly OBs were dissolved with DAS buffer (0.1 M Na_2CO_3, 0.15 M NaCl, 10 mM EDTA,
293 pH 11), and DNA was then extracted from the liberated occlusion-derived virus particles using a
294 DNA isolation kit (Omega Bio-tek) following the manufacturer's instructions. For the BAC, DNA
295 was extracted from 50 ml LB from an overnight culture using a plasmid midi kit (Qiagen).
296 Successful genomic DNA extraction was confirmed by PCR with primers gp41 inner F (5'-
297 CAAGAGCAAAGAACCGACG-3') and inner R (5'-TTATGCAGTGCGCCCTTTCGT-3'), and
298 contamination of SeMNPV was ruled out by PCR with primers Se F (5'-
299 GACGACGAATTATGTTGTGACCGAC-3') and R (5'- AGATGGATGGAAAGGCAACGCT-3').
300 Purified DNA (~ 1.5 ug) from the evolved AcMNPV lineages A, B, C, D and E, as well as the

301 ancestral BAC, was sequenced by Illumina HiSeq PE150 (Beijing Novogene Bioinformatics

302 Technology Co., Ltd).

303 **Table 3:** Parameters for the models for estimating mutation rates

Fixed or fitted parameter	Parameter	Value	Explanation
Fixed	g	11,646	The length of the neutral bacmid region in bases.
		145,465	The length of the full genome, including the neutral bacmid region.
	λ	46	The bottleneck size for the viral founding population in each insect larvae. Following [44], the bottleneck size is related to the host survival (S) for AcMNPV infection of *S. exigua:* $\lambda = \ln(S)$. For each insect exposed to 10 x LD_{99} dose: $\lambda = 10 * \ln(1 - 0.99) \sim 46$.
	κ	5.32×10^{8}	The final size of the virus population within a single host insect. As AcMNPV generates OBs with multiple occlusion derived viruses (ODVs), and ODVs with multiple nucleocapids, each containing single copy of the genome. The mean OB yield per larvae during the experiment was $1.33*10^{6}$, based on the OB concentrations measured for each pool of five insects made after each round of passaging, assuming 100 ODV per OB (we are not aware of any empirical estimates) and 4 nucleocapsids per ODV [45].
	σ	1001	Parameter value minus one indicates the max. number of mutations per genome allowed in the simulations.
	φ	10^{4}	Threshold value of population growth for switching from stochastic to deterministic mutation.
	τ	0.5%, 1%, 2%	Minimum frequency for the detection of mutations, indicated as a percentage.
Fitted	ρ	1, 3, 10	Parameter that describes the viral mode of replication, with 1 being equivalent to equivalent to “geometric growth” by fission and large values (i.e., 10) representing “stamping machine” replication kinetics.
	$\log_{10}\mu$	-10, -9.9, -9.8, [...], -5	Mutation rate (s/n/r)

304 *Mutation calling and filtering*

305 Because the number of viral reads was not equal across samples, fastq files were subsampled to
306 ensure an approximately equal mean coverage across the reference genome for each isolate
307 using seqtk sample [41]. NGS data was analyzed using CLC Genomics Workbench 20.0 [42].
308 Reads were trimmed (quality limit = 0.05) and mapped to the reference genome (see Online
309 Materials for sequence and annotation files). Mutations were called using the “low frequency
310 variant detection tool” (minimum frequency = 0.5%). An overview of parameter settings can be
311 found in the Supplementary Online Materials (Appendix 1).

312 Due to the small likelihood of the same mutation occurring independently in two or more
313 populations, we assume mutations found in two or more evolved populations were present in the
314 ancestral population (having been present at low frequency in the BAC DNA or occurring *de novo*
315 after reconstitution of the virus. Therefore, mutations called in multiple lineages and/or in the
316 ancestral BAC isolate were filtered out. Additional filtering criteria were: forward-reverse balance
317 > 0.05, read count > 10, and the type of mutation is "SNV" (single nucleotide variant). Additionally,
318 positions with extreme coverage values were excluded. To this end, we ranked the coverage
319 value per position for each lineage and excluded the upper and lower 1%. Analyses were done
320 with three thresholds (τ) for mutation frequency: 0.5%, 1% and 2% (see Supplementary Online
321 materials, Appendices 2-4). Finally, mutations were tallied per isolate, both across the whole
322 genome and for the neutral bacmid insert.

323 *Mutation model and mutation rate estimation*

324 We generated a stochastic model that predicts the distribution of mutation frequencies per base
325 in an evolving virus genome, and then fitted this model to our empirical data with a maximum
326 likelihood approach to obtain mutation rate estimates. The model was implemented in R 4.0.3
327 [43] and all code is available (see Supplementary Online Material, Appendices 5-6). We model

328 the genome region under consideration as a vector with *g* elements for each nucleotide position,
329 with each element representing the total frequency *f* of mutated bases at position *i*. For simplicity,
330 we do not consider the identity of the mutated bases and we do not allow for reversions, as we
331 are considering scenarios in which mutations are rare and the probability of a reversion occurring
332 and reaching high frequency is very low. We assume that all mutations are strictly neutral, and
333 that all changes in mutation frequency result from the occurrence of *de novo* mutations or neutral
334 processes like stochastic changes in allele frequencies due to population bottlenecks (i.e. genetic
335 drift). All model parameter values are given in Table 3, together with additional explanation and
336 justification.

337 At the start of the infection of an individual host, there is a bottleneck with λ virus genomes
338 initiating infection. For each position in the genome, we draw the number of genomes containing
339 a mutation at this position from a binomial distribution, where for the ith position: $P(X_i = x_i) = \binom{\lambda}{x_i}$
340 $f_i^{x_i}(1-f_i)^{\lambda-x_i}$, where X is the number of mutant genomes added to the population at a particular
341 step in the infection process (and *f* is the frequency of mutated bases at position *i*). We obtained
342 an estimate of λ = 46 by considering the relationship between host mortality and the number of
343 viral founders [44] (see Table 3). The virus population then expands within the host exponentially
344 with a replication factor ρ per cycle of virus replication within the host, such that $N_t = \lambda(1+\rho)^t$
345 where *N* is the number of genomes present at a time *t*, measured in generations of viral replication
346 within the host. It is unknown what the mode of replication [30,31] is for a baculovirus. We
347 therefore used values of 1 ("geometric" or "symmetric" replication with a doubling of the number
348 of copies per cycle – one original genome copy and one replicated copy), 3 ("mixed" replication –
349 one original genome copy and three replicated copies) and 10 ("stamping machine" or
350 "asymmetric" replication) for ρ. Replication proceeds until the carrying capacity κ of a host is
351 reached, with an expansion to exactly κ virus genomes allowed in the final round of replication.
352 During each round of replication, the number of new mutants that occur at each position follows

353 a binomial distribution, such that the mutation rate μ is the probability of success and η, the number
354 of genomes generated during that round of replication which are not mutated at this nucleotide
355 position (i.e., $\eta_{i,t} = \rho N_{t-1}(1 - f_{i,t-1})$), is the number of events: $P(X_{i,t} = x_{i,t}) = \binom{\eta_{i,t}}{x_{i,t}} \mu^{x_{i,t}} (1-\mu)^{\eta_{i,t} - x_{i,t}}$.
356 However, to make the model computationally tractable for large population sizes, we switched to
357 deterministic mutation (I.e., $X_{i,t} = \eta_{i,t}\mu$) once a large number of virus genomes was being
358 generated relative to the mutation rate ($N_t\varphi > \mu^{-1}$), where φ is a constant. Note that all mutations
359 are assumed to be neutral and that the bottleneck at the start of infection is narrow (λ = 46).
360 Mutations occurring late in infection when the viral census population size is large therefore will
361 rarely be sampled during the bottleneck events at the start of the next round of infection (i.e. serial
362 transfer). To model the infection of five host larvae per replicate, we simulated five separate
363 infections and pooled the viral progeny by taking the mean mutation frequency per site over the
364 five larvae for each position in the genome, and using these f_i values for the next round of infection.
365 To fit the model to the data, we first ran 1000 simulations for each combination of
366 parameter values (i.e., μ, ρ and τ) to generate model predictions. We compared the observed
367 number of experimental replicates (q_j) with $j - 1$ mutated nucleotide positions with a frequency f_i
368 higher than the threshold value τ, to the frequency predicted by the model (β_j). (I.e., q_1 is the
369 number of experimental replicates with 0 nucleotide positions for which $f_i > \tau$, q_2 is the number of
370 replicates with 1 nucleotide positions for which $f_i > \tau$, etc.) The multinomial pseudo-likelihood of
371 any realization is then: $P(\beta_1 = q_1, \beta_2 = q_2, [\ldots], \beta_\sigma = q_\sigma) = \frac{q!}{\prod_{j-1}^{\sigma} q_j!} \prod_{j-1}^{\sigma} \beta_j^{q_j}$, where σ-1 = 1000 is the
372 maximum number of mutated bases that were tracked in the simulations. If any values of β
373 exceeded σ-1 in any simulation, results from that set of parameter values were excluded from
374 further analysis. We fitted the model to 1000 bootstrapped datasets to determine the 95%
375 confidence interval of the parameter estimates.
376

377 *Mutation rate estimates with established approaches*

378 We estimated the mutation rate with an established approach, to compare to the estimates made
379 with our simulation-model approach. A canonical approach [9] for calculating mutation rate (s/n/r)
380 is $\mu = \frac{3m_s}{T_s c\alpha}$, where m_s is the number of observed mutations observed in sequenced clones, T_s is
381 the mutational target size, c is the number of viral generations, and α is a correction for the effects
382 of selection. To obtain m_s from our deep sequencing data, we sum the frequency of all observed
383 mutations (f_i) above the threshold for mutation selection τ in all lineages. If these sequencing data
384 are accurate and mutations are neutral, the frequency of each mutation is also the probability that
385 this mutation would be detected in a randomly selected clone by sequencing. This approach is a
386 simple approximation, as here we do not consider the effect of the threshold for mutation detection
387 (τ) on mutation rate estimates. (Lowering τ will lead to a larger number of mutations and
388 consequently a higher mutation rate estimate. To keep this method as simple as possible and
389 free of additional assumptions, we choose not to incorporate any corrections.) Note that because
390 we sum the frequency of all possible mutations over each site, we can drop the three in the
391 numerator. To obtain T_s, we multiply the length of the neutral region by the number of replicates.
392 To obtain c we estimate the number of generations assuming different values for ρ (i.e., 1, 3 and
393 10 as for the simulation-based model fitting), such that $c = \theta \cdot ln(\kappa/\lambda)/ln(1+\rho)$, where θ is the
394 number of passages. Finally, we can drop α because we only consider mutations in the neutral
395 bacmid region. One-thousand bootstrapped datasets were used to obtain fiducial limits for the
396 mutation rate estimates.

397 *dI/dS and dN/dS analyses*

398 Estimates of dN/dS (i.e., the normalized rate of nonsynonymous mutations, here made for
399 authentic viral genes) were made using standard methods [46,47]. As we are not aware of any

400 estimates of the mutation spectrum for insect DNA viruses and our own data suggest these biases
401 may not be very strong (Table 2), we assume no mutation bias is present (i.e., a transition to
402 transversion ratio of 1). For the dI/dS [3], the dS term is the same as for the dN/dS analysis,
403 derived from the results for authentic viral genes. The dI term is determined for mutations in the
404 bacmid neutral region. Ninety-five percent confidence intervals of the dI/dS and dN/dS were
405 obtained using 1000 bootstrapped datasets, and data were tested for significance with a one-
406 sample *t*-test on the dN/dS values calculated for individual samples compared to a test value of
407 1. However, when $\tau > 0.5\%$ for one or more samples the number of synonymous samples was 0,
408 and hence these analyses could only be performed for $\tau = 0.5\%$. Full results and R code are
409 available in the Supplementary Online Information (Appendices 7-9).

410 **Acknowledgements**

411 The authors thank Yue Han and Marleen Henkens for technical assistance. G.A. was supported
412 by the Netherlands Fellowship Program PhD Grant No. CF7554/2011 (Nuffic, www.nuffic.nl).
413 MPZ was supported by a VIDI grant from the Netherlands Organization for Scientific Research
414 Grant No. 016.VIDI.171.061 (NWO, www.nwo.nl).

415 The funders had no role in study design, data collection and analysis, decision to publish, or
416 preparation of the manuscript. The authors have declared that no competing interests exist.

417 **References**

418 1. de Visser JAGM, Krug J. Empirical fitness landscapes and the predictability of evolution.
419 Nat Rev Genet. 2014;15: 480-490.

420 2. Bull JJ, Badgett MR, Wichman HA, Huelsenbeck JP, Hillis DM, Gulati A, et al.
421 Exceptional convergent evolution in a virus. Genetics. 1997;147: 1497–1507.

422 3. Tenaillon O, Rodriguez-Verdugo A, Gaut RL, McDonald P, Bennett AF, Long AD, et al.
423 The molecular diversity of adaptive convergence. Science. 2012;335: 457–461.

424 4. Sprouffske K, Aguílar-Rodríguez J, Sniegowski P, Wagner A. High mutation rates limit

425 evolutionary adaptation in *Escherichia coli*. PLOS Genet. 2018;14: 1-31.

426 5. Van Dijk T, Hwang S, Krug J, De Visser JAGM, Zwart MP. Mutation supply and the
427 repeatability of selection for antibiotic resistance. Phys Biol. 2017;14: 055005.

428 6. Salverda MLM, Koomen J, Koopmanschap B, Zwart MP, De Visser JAGM. Adaptive
429 benefits from small mutation supplies in an antibiotic resistance enzyme. Proc Natl Acad
430 Sci U S A. 2017;114: 12773-12778.

431 7. Peck KM, Lauring AS. Complexities of viral mutation rates. J Virol. 2018;92: 1–8.

432 8. Hughes D, Andersson DI. Evolutionary trajectories to antibiotic resistance. Annu Rev
433 Microbiol. 2017;71: 579–596.

434 9. Sanjuán R, Nebot MR, Chirico N, Mansky LM, Belshaw R. Viral mutation rates. J Virol.
435 2010;84: 9733–9748.

436 10. Sanjuán R, Domingo-Calap P. Mechanisms of viral mutation. Cell Mol Life Sci. 2016;73:
437 4433–4448.

438 11. Luria SE. The frequency distribution of spontaneous bacteriophage mutants as evidence
439 for the exponential rate of phage reproduction. Cold Spring Harb Symp Quant Biol.
440 1951;16: 463–470.

441 12. Pauly MD, Procario MC, Lauring AS. A novel twelve class fluctuation test reveals higher
442 than expected mutation rates for Influenza A viruses. Elife. 2017;6: 1–18.

443 13. Sanjuan R, Moya A, Elena S. The distribution of fitness effects caused by single-
444 nucleotide substitutions in an RNA virus. Proc Natl Acad Sci USA. 2004;101: 8396–8401.

445 14. Carrasco P, de la Iglesia F, Elena SF. Distribution of fitness and virulence effects caused
446 by single-nucleotide substitutions in Tobacco etch virus. J Virol. 2007;81: 12979–12984.

447 15. Mahmoudabadi G, Phillips R. A comprehensive and quantitative exploration of thousands
448 of viral genomes. Elife. 2018;7: 1–26.

449 16. Knopf CW. Evolution of viral DNA-dependent DNA polymerases. Virus Genes. 1998;16:
450 47–58.

451 17. Gago S, Elena SF, Flores R, Sanjuán R. Extremely high mutation rate of a hammerhead
452 viroid. Science. 2009;323: 1308.

453 18. Haase S, Sciocco-Cap A, Romanowski V. Baculovirus insecticides in Latin America:
454 Historical overview, current status and future perspectives. Viruses. 2015;7: 2230-2267.

455 19. van Oers MM. Opportunities and challenges for the baculovirus expression system. J
456 Invertebr Pathol. 2011;107: S3–S15.

457 20. Harrison R, Herniou E, Jehle J, Theilmann D, Burand J, Becnel J, et al. ICTV virus
458 taxonomy profile: Baculoviruses. J Gen Virol. 2018;99: 1185–1186.

459 21. Smith IR, Crook NE. In vivo isolation of baculovirus genotypes. Virology. 1988;166: 240–

460 244.

461 22. Cory JS, Green BM, Paul RK, Hunter-Fujita F. Genotypic and phenotypic diversity of a
462 baculovirus population within an individual insect host. J Invertebr Pathol. 2005;89: 101–
463 111.

464 23. Kennedy DA, Dwyer G. Effects of multiple sources of genetic drift on pathogen variation
465 within hosts. PLoS Biol. 2018;16: e2004444.

466 24. Chateigner A, Bézier A, Labrousse C, Jiolle D, Barbe V, Herniou EA. Ultra deep
467 sequencing of a baculovirus population reveals widespread genomic variations. Viruses.
468 2015;7: 3625–3646.

469 25. Sanjuán R, Agudelo-Romero P, Elena SF. Upper-limit mutation rate estimation for a plant
470 RNA virus. Biol Lett. 2009;5: 394–396.

471 26. Tromas N, Elena SF. The rate and spectrum of spontaneous mutations in a plant RNA
472 virus. Genetics. 2010;185: 983–989.

473 27. Luckow VA, Lee SC, Barry GF, Olins PO. Efficient generation of infectious recombinant
474 baculoviruses by site-specific transposon-mediated insertion of foreign genes into a
475 baculovirus genome propagated in *Escherichia coli*. J Virol. 1993;67: 4566–4579.

476 28. Willemsen A, Zwart MP. On the stability of sequences inserted into viral genomes. Virus
477 Evol. 2019;5: 1–16.

478 29. Sardanyés J, Solé R V., Elena SF. Replication mode and landscape topology
479 differentially affect RNA virus mutational load and robustness. J Virol. 2009;83: 12579–
480 12589.

481 30. Martínez F, Sardanyés J, Elena SF, Daròs JA. Dynamics of a plant RNA virus
482 intracellular accumulation: Stamping machine vs. geometric replication. Genetics.
483 2011;188: 637–646.

484 31. Schulte MB, Draghi JA, Plotkin JB, Andino R. Experimentally guided models reveal
485 replication principles that shape the mutation distribution of RNA viruses. Elife. 2015;4: 1–
486 18.

487 32. Leisy DJ, Rohrmann GF. Characterization of the replication of plasmids containing *hr*
488 sequences in baculovirus-infected *Spodoptera frugiperda* cells. Virology. 1993;196: 722–
489 730.

490 33. Sanjuan R. Viral mutation rate estimates. [cited 26 Feb 2021]. Available:
491 http://www.uv.es/rsanjuan/virmut

492 34. Blanco L, Bernad A, Blasco MA, Salas M. A general structure for DNA-dependent DNA
493 polymerases. Gene. 1991;100: 27–38.

494 35. Tomalski MD, Wu J, Miller LK. The location, sequence, transcription, and regulation of a
495 baculovirus DNA polymerase gene. Virology. 1988;167: 591–600.

496 36. Hang X, Guarino LA. Purification of Autographa californica nucleopolyhedrovirus DNA
497 polymerase from infected insect cells. J Gen Virol. 1999;80: 2519–2526.

498 37. Karam JD, Konigsberg WH. DNA polymerase of the T4-related bacteriophages. Prog
499 Nucleic Acid Res Mol Biol. 2000;64: 65-96.

500 38. Acevedo A, Brodsky L, Andino R. Mutational and fitness landscapes of an RNA virus
501 revealed through population sequencing. Nature. 2014;505: 686-690.

502 39. Simon O, Williams T, Caballero P, Lopez-Ferber M. Dynamics of deletion genotypes in
503 an experimental insect virus population. Proc R Soc B: Biol Sci. 2006;273: 783-790.

504 40. Clavijo G, Williams T, Simon O, Munoz D, Cerutti M, Lopez-Ferber M, Caballero P.
505 Mixtures of complete and *pif1*- and *pif2*-deficient genotypes are required for increased
506 potency of an insect nucleopolyhedrovirus. J Virol. 2009;83: 5127-5136.

507 41. Anonymous. Seqtk: Toolkit for processing sequences in FASTA/Q formats. [cited July 7
508 2021] Available: https://github.com/lh3/seqtk.

509 42. Anonymous. CLC Genomics Workbench 20.0. [cited 8 Apr 2021]. Available:
510 https://digitalinsights.qiagen.com

511 43. The R Foundation for Statistical Computing. R: A language and environment for statistical
512 computing. Vienna, Austria; 2020.

513 44. Zwart MP, Hemerik L, Cory JS, de Visser JAGM, Bianchi FJJA, van Oers MM, Vlak JM,
514 Hoekstra RF, van der Werf W. An experimental test of the independent action hypothesis
515 in virus-insect pathosystems. Proc R Soc B: Biol Sci. 2009;276: 2233–42.

516 45. Zwart MP, van Oers MM, Cory JS, van Lent JWM, van der Werf W, Vlak JM.
517 Development of a quantitative real-time PCR for determination of genotype frequencies
518 for studies in baculovirus population biology. J Virol Methods. 2008;148: 146–54.

519 46. Yang Z, Bielawski JR. Statistical methods for detecting molecular adaptation. Trends Ecol
520 Evol. 2000;15: 496–503.

521 47. Zwart MP, Ali G, van Strien EA, Schijlen EGWM, Wang M, van der Werf W, et al.
522 Identification of loci associated with enhanced virulence in Spodoptera litura
523 nucleopolyhedrovirus isolates using deep sequencing. Viruses. 2019;11: 1–13.

Appendix

Table S1: Relative frequencies of mutations observed per type, for the whole genome and bacmid only datasets, across mutation frequency threshold values (τ), given as a percentage.

	Relative frequency of mutation				
	Whole genome			Bacmid only	
Mutation	τ = 0.5 (n=69)	τ = 1 (n=20)	τ = 2 (n=8)	τ = 0.5 (n=9)	Mutation type
CA	0.174	0.250	0.125	0.111	Transversion
CG	0.014	0.000	0.000	0.000	Transversion
TA	0.043	0.000	0.000	0.000	Transversion
TG	0.014	0.000	0.000	0.111	Transversion
AC	0.043	0.000	0.000	0.111	Transversion
AT	0.058	0.000	0.000	0.111	Transversion
GC	0.029	0.000	0.000	0.000	Transversion
GT	0.217	0.300	0.125	0.111	Transversion
GA	0.130	0.200	0.250	0.222	Transition
CT	0.101	0.150	0.250	0.111	Transition
TC	0.072	0.050	0.125	0.000	Transition
AG	0.101	0.050	0.125	0.111	Transition

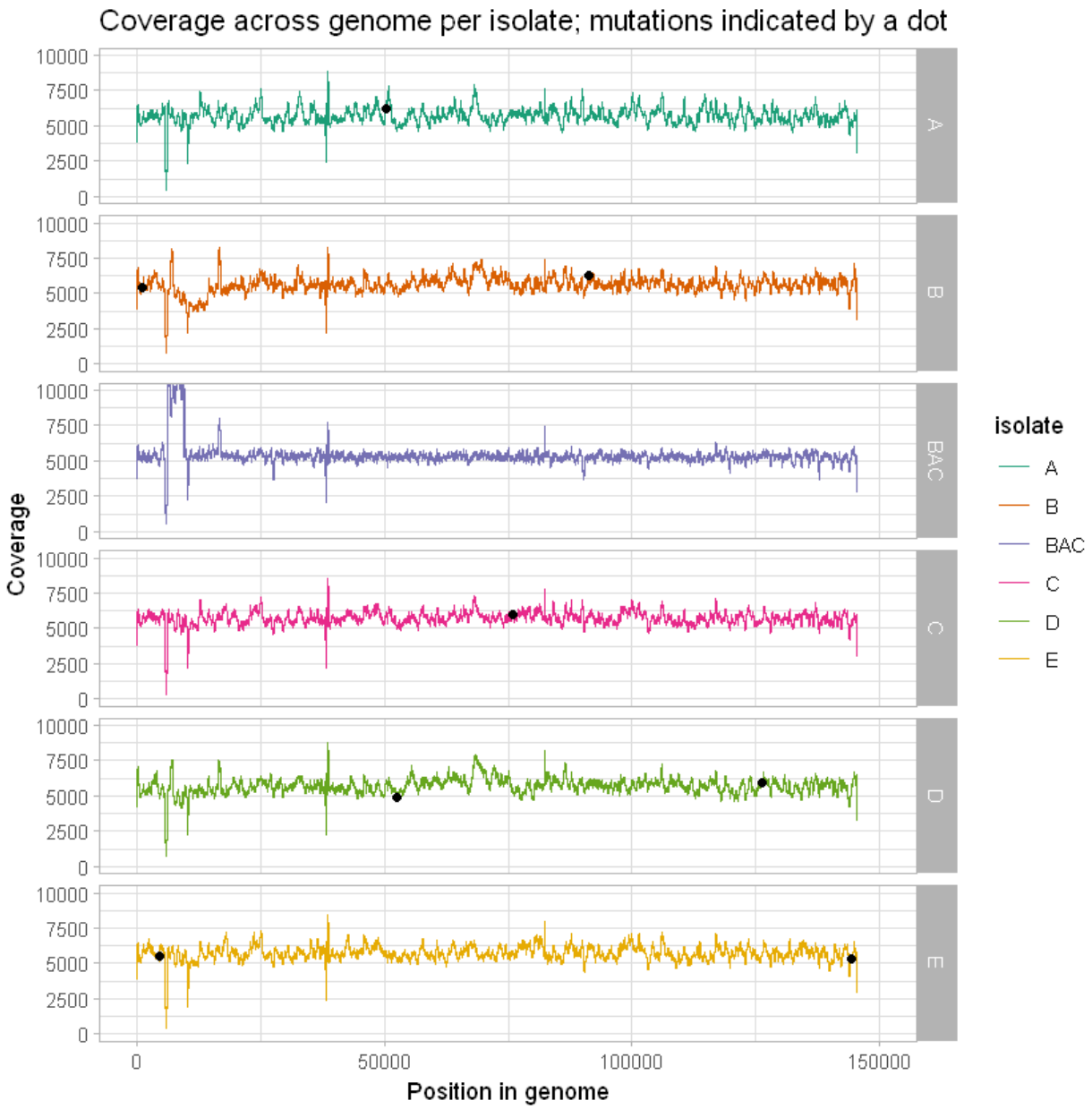

Figure S1: We show coverage along the genome for each evolved line (A, B, C, D and E) as well as ancestral strain BAC. Position of mutations observed at mutation frequency threshold value (τ) = 2 are shown as black dots. Coverage patterns are similar between the different isolates. The peak observed at around 10000 bp for the BAC isolate is due to the presence of empty bacmid vectors in sequencing data and is omitted from mutation calling.

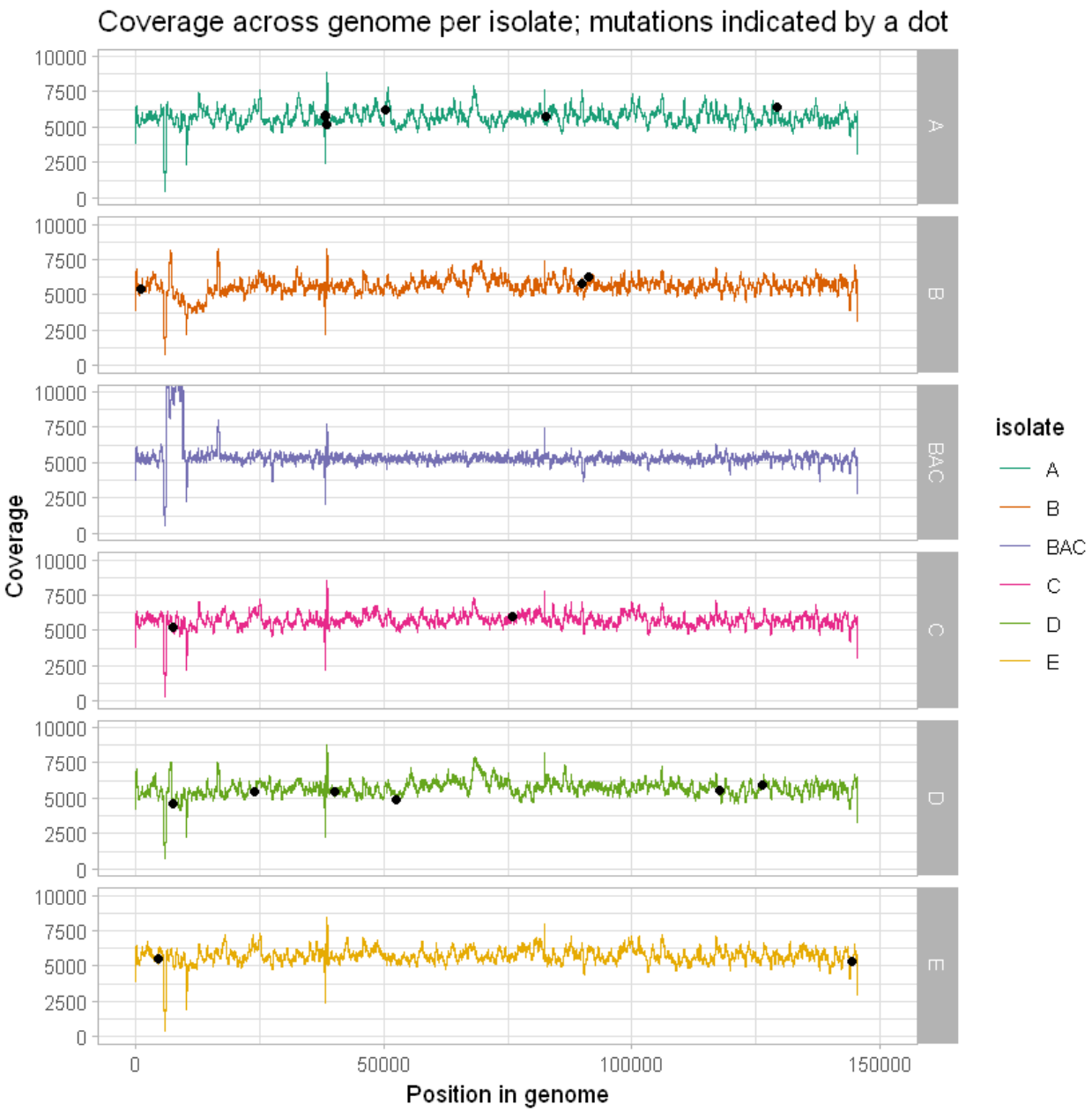

Figure S2: We show coverage along the genome for each evolved line (A, B, C, D and E) as well as ancestral strain BAC. Position of mutations observed at mutation frequency threshold value (τ) = 1 are shown as black dots. Coverage patterns are similar between the different isolates. The peak observed at around 10000 bp for the BAC isolate is due to the presence of empty bacmid vectors in sequencing data and is omitted from mutation calling.

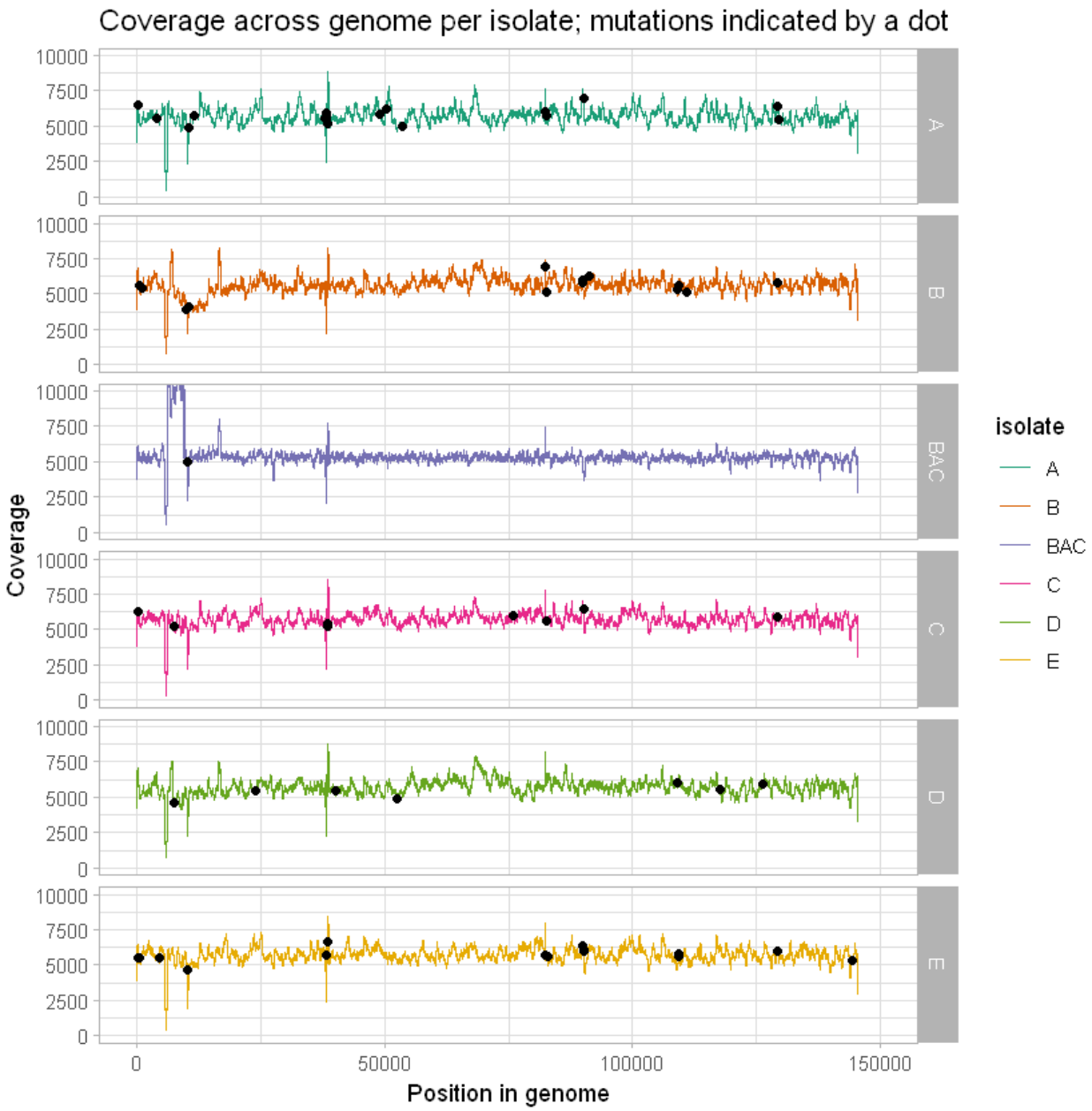

Figure S3: We show coverage along the genome for each evolved line (A, B, C, D and E) as well as ancestral strain BAC. Position of mutations observed at mutation frequency threshold value (τ) = 0.5 are shown as black dots. Coverage patterns are similar between the different isolates. The peak observed at around 10000 bp for the BAC isolate is due to the presence of empty bacmid vectors in sequencing data and is omitted from mutation calling.

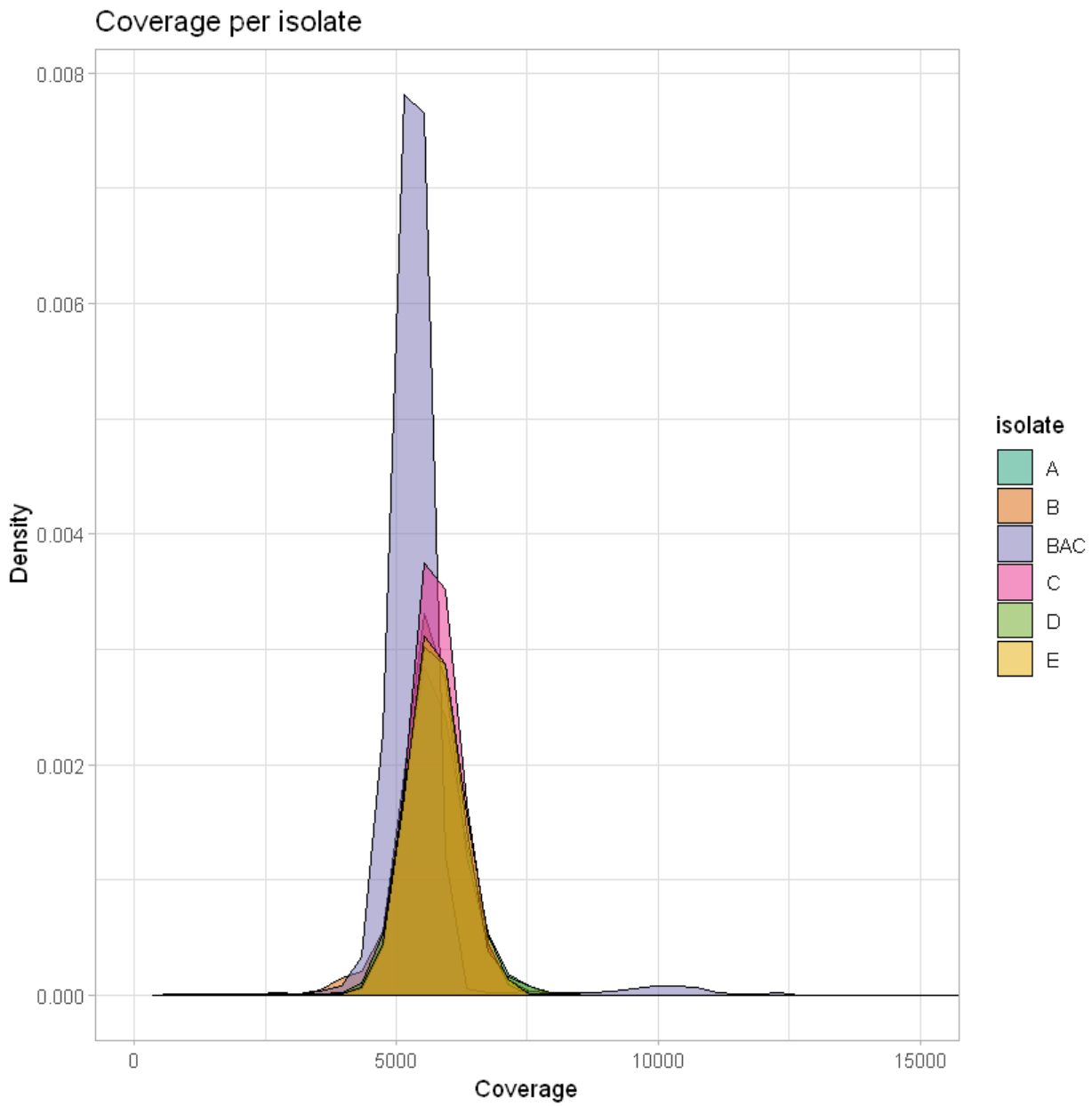

Figure S4: Coverage distribution per isolate after subsampling to approximately equal mean coverage. Isolates have a mean coverage of around 5500. The BAC isolate is showing an additional peak at a coverage of around 10000, which is explained by the presence of empty bacmid vectors in sequencing data.

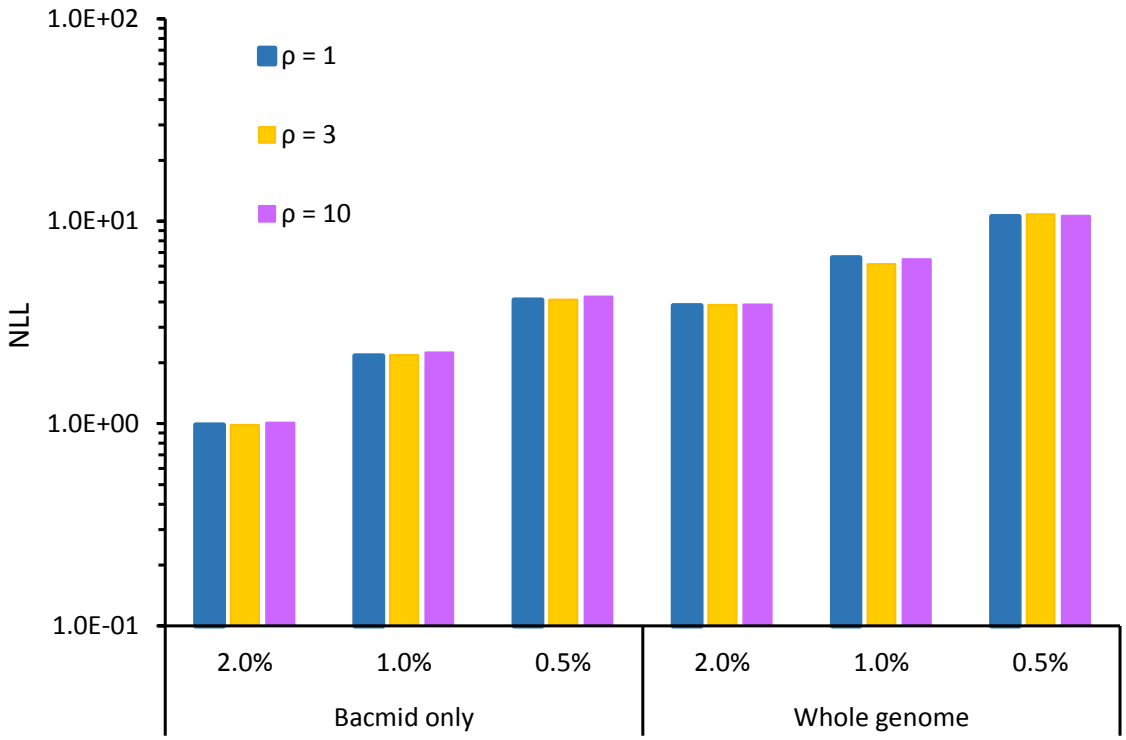

Figure S5: We show the negative log likelihood (NLL) for models fitted with different mutation frequency threshold values (τ), given as a percentage. Mutation frequency threshold values clearly effect model fit, as they have an effect on the number of mutations that will be detected. By contrast, assumptions on the value for the parameter that determines the mode of virus replication (ρ) had little effect on model fit. This result is not surprising however, given that our model does not consider the frequency of mutations, but simply the number of bases with a mutation frequency greater than τ.

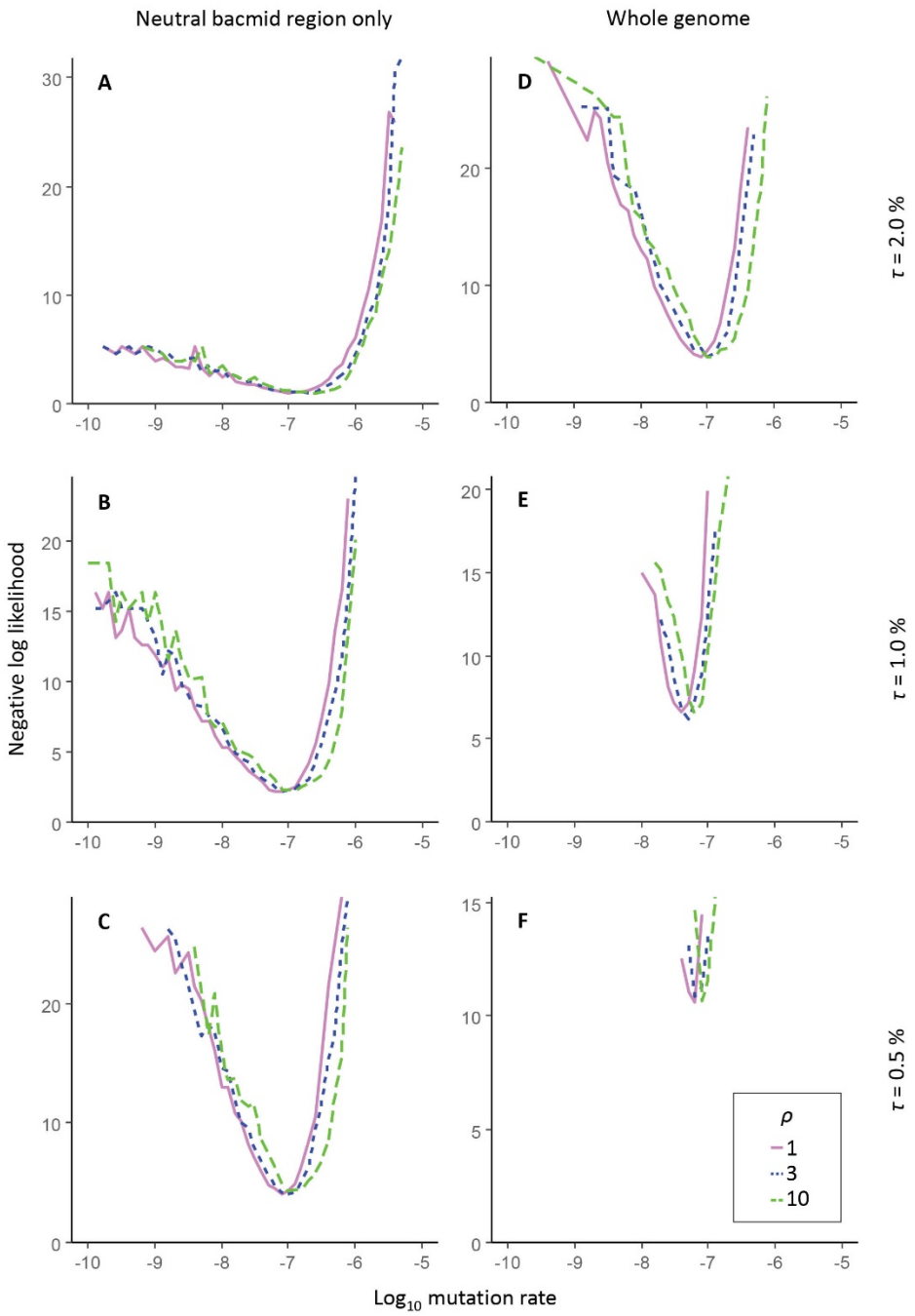

Figure S6: Results of the fitting of the simulation model to the experimental data, for making mutation rate estimates. For all panels, the abscissa is the $\log_{10}$ mutation rate and the originate the negative log likelihood. Panels on the left correspond to the neutral bacmid region data, and panels on the right to the whole genome data. Different thresholds for the detection of mutations (τ) were also employed, ranging from 0.5% (bottom row) to 1% (middle row) to 2% (top row). The different colors and line types indicate model fit for different values of ρ, the parameter that describes the viral mode of replication. Whereas higher values of ρ lead to lower mutation rate estimates, this model parameter does not impact the minimum for the NLL.

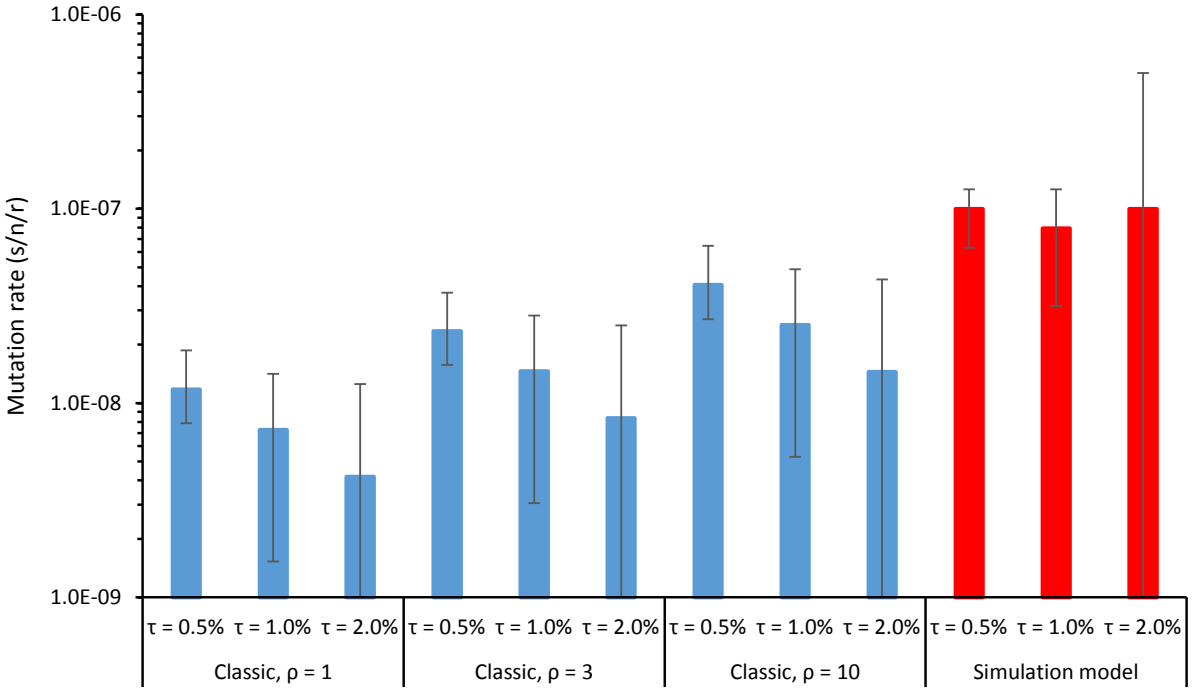

Figure S7: Estimate of mutation rate (s/n/r) using established methods applied to deep sequencing data (blue bars, samples categorized as "Classic"), as an alternative to our approach using a simulation-based model (red bars, samples categorized as "Simulation model"). Mutation rates were estimated for different values of the viral mode of replication (ρ) and with different values for the threshold of mutation detection (τ). Error bars represent the 95% fiducial limits, as determined by bootstrapping. When the lower fiducial limit extends beyond the lower limit of the axis, this indicates a lower fiducial limit of zero. Overall, these estimates were lower than those obtained with the approach employing a simulation model. As baculoviruses most likely employ rolling circle amplification, replication is likely to have a high value of ρ. Furthermore, this method is clearly sensitive to differences in the mutation detection threshold, as the cumulative frequency of mutations above this value is used required to estimate mutations and no correction is made for this threshold. Therefore, the best estimates with this approach assume the highest value of ρ and the lowest mutation detection thresholds (τ), provided all mutations are assumed to be bona fide. The estimate for these conditions (τ = 0.5% and ρ = 10), renders an estimate of $\mu = 4 \times 10^{-8}$ which is lower but roughly similar than for our simulation-based approach ($\mu \sim 10^{-7}$).